A Simple Mechanical Model for Molecular Geometry Based on the Hellmann–Feynman Theorem. I. General Principles and Applications to AH₂, AH₃, AH₄, AB₂, HAB, and ABC Molecules†

B. M. Deb

Contribution from the Department of Chemistry, Indian Institute of Technology, Bombay, India. Received October 7, 1972

Abstract: A new model for molecular geometry, based on qualitative interpretations drawn from the Hellmann–Feynman theorem, is proposed. The model regards molecular shapes to be determined primarily by the electrostatic "pull" on the terminal nuclei by the electron–nuclear attractive forces arising from the one-electron density in an occupied MO. It is postulated that the gross equilibrium molecular geometry is governed mainly by the behavior of the highest occupied molecular orbital (HOMO). By adopting certain heuristic rules for the qualitative construction of low-lying symmetry-adapted polycenter LCAO–MO's (using only a valence sp basis), for arranging these MO's in energy order, and for deciding the nature of the transverse electron–nuclear forces acting on the terminal nuclei, Walsh type predictions about gross equilibrium shapes have been made for the above six molecule classes. The predictions hold true even if one replaces the nonhydrogenic atoms by groups of atoms. Using the HOMO postulate the bond angle and bond length variations from molecule to molecule within a class can also be predicted. The model is flexible enough to incorporate the phenomenon of internal motions, the distortions in molecular geometry due to the static Jahn–Teller effect, as well as the transferability in geometry predictions from smaller to higher molecule classes. The HOMO is likely to provide a simple unifying principle in chemistry for understanding the structure and reactivity of molecules.

1. Introduction

An understanding about the shapes of molecules in their ground and excited/ionized states is essential for explaining and correlating their various physical, chemical, and biological properties. The crux of the problem is to explain how a given group of atoms, in the course of molecule formation, arranges itself in a specific geometric pattern and not in any other. Over the years a number of qualitative models have emerged to account for a host of molecular shapes.[1-8] In this paper we propose a simple mechanical model whose main objective is to provide a pictorial description of and a physical insight into how gross equilibrium molecular shapes come about in the three-dimensional space.

The proposed model regards molecular shapes to be determined primarily by the electrostatic "pull" on the terminal nuclei by the electron–nuclear attractive forces generated by the one-electron density in an oc-

† NOTE ADDED IN PROOF. This and the following paper (part II) are dedicated to the memory of Professor C. A. Coulson who passed away on Jan. 7, 1974. Charles Coulson was an extraordinary man behind whose penetrating blue eyes lay a deep well of compassion for other human beings. For those who knew him, something wonderful and sweet seems to have gone out of their lives.

(1) L. Pauling, "The Nature of the Chemical Bond," Cornell University Press, Ithaca, N. Y., 1960, Chapter 4; C. S. Sharma, *Indian J. Pure Appl. Phys.*, **8**, 15 (1970).

(2) A. D. Walsh, *J. Chem. Soc.*, 2260, 2266, 2288, 2296, 2301, 2306, 2321 (1953); *Annu. Rep. Progr. Chem.*, **61**, 8 (1964); see also Y. Takahata, G. W. Schnuelle, and R. G. Parr, *J. Amer. Chem. Soc.*, **93**, 784 (1971).

(3) R. J. Gillespie, *Angew. Chem.*, **6**, 819 (1967); see also H. B. Thompson, *J. Amer. Chem. Soc.*, **93**, 4609 (1971).

(4) J. W. Linnett, "Electronic Structure of Molecules," Methuen, London, 1964.

(5) (a) W. F. Luder, "The Electron-Repulsion Theory of the Chemical Bond," Reinhold, New York, N. Y., 1967; (b) A. W. Searcy, *J. Chem. Phys.*, **28**, 1237 (1958); 30, 1635 (1959); 31, 1 (1959).

(6) L. S. Bartell, *J. Chem. Educ.*, **45**, 754 (1968); H. A. Bent, *ibid.*, 45, 768 (1968); 43, 170 (1966); 42, 302, 348 (1965); 40, 446, 523 (1963).

(7) J. J. Kaufman, *Int. J. Quantum Chem., Symp.*, **1**, 261, 485 (1967).

(8) (a) R. G. Pearson, *J. Amer. Chem. Soc.*, **91**, 4947 (1969); *J. Chem. Phys.*, **52**, 2167 (1970); (b) G. W. Schnuelle and R. G. Parr, *J. Amer. Chem. Soc.*, **94**, 8974 (1972).

cupied MO. Such forces can be obtained from the electrostatic Hellmann–Feynman (H–F) theorem.

$$F_{px} = -\sum_{p<q} \frac{Z_p Z_q}{R_{pq}^2} \frac{\partial R_{pq}}{\partial X_p} + Z_p \int \rho(r) \frac{x_p}{r_p^3} d\tau \quad (1)$$

where F_{px} is the x component of the net force acting on the pth nucleus in a molecule and is the balance of a nuclear–nuclear repulsion term and an electron–nuclear attraction term. In eq 1 X_p is the x coordinate of the pth nucleus, Z_p its nuclear charge, R_{pq} an internuclear distance, and $\rho(r)$ the total one-electron density at the point r; the integration in eq 1 is to be done in three-dimensional space and x_p and r_p are position coordinates in space measured from the pth nucleus (see ref 9 for a review on the H–F theorem and its chemical applications). Further, in eq 1 we have adopted the convention[10] of taking attractive forces as positive and repulsive forces as negative. If one uses a single-configurational LCAO–MO wave function then the required single-particle density is

$$\rho(r) = \sum_i n_i \phi_i^2(r) \quad (2)$$

where ϕ_i is a real MO occupied by η_i electrons. The electron–nuclear component of the net force in eq 1 thus becomes

$$Z_p \sum_i \eta_i \langle \phi_i | x_p / r_p^3 | \phi_i \rangle \quad (3)$$

The quantity within the summation sign in (3) represents the x component of the electronic force on the nucleus p due to a one-electron MO and is of central interest to us in this paper.

For predicting the shapes in a given class of molecules the procedure adopted here consists of three steps.

(1) Construction of low-lying symmetry-adapted polycenter LCAO–MO's, according to certain heuristic

(9) B. M. Deb, *Rev. Mod. Phys.*, **45**, 22 (1973).

(10) (a) C. A. Coulson and B. M. Deb, *Int. J. Quantum Chem.*, **5**, 411 (1971); (b) C. A. Coulson and B. M. Deb, *Mol. Phys.*, **16**, 545 (1969).

rules (see next section), using only valence s and p AO's as basis functions. We then use another set of heuristic rules (see next section) to arrange these MO's in a proper energy sequence.

(2) Pictorial representation of the constructed MO's and a prescription (see next section) to decide whether an MO density favors an increase or a decrease in magnitude of a geometrical parameter. For this one first considers a physical model for nuclear motions as well as the direction of the force tending to produce such motions, leading to an equilibrium geometry.

(3) The prediction of shapes depending on the number of valence electrons in a molecule. This is arrived at with the help of the following postulate and by looking at the *direction* of a transverse component of the electron–nuclear attractive force acting on a terminal nucleus and generated by an occupied MO.

Postulate HOMO. The gross equilibrium geometry of a molecule is determined primarily by the behavior of the highest occupied (or outermost) molecular orbital (HOMO), when nondegenerate, with respect to the geometrical parameter (angle or length) examined. In case the HOMO is insensitive with regard to a valence angle the angular behavior of the next lower MO, if sensitive, will determine the shape; if this MO is insensitive too then the next lower MO is to be examined and so on.

However, there might be two cases where it may not be possible to distinguish a unique HOMO. (a) The molecular electronic state is orbitally degenerate. In this case the orbital to be filled last, if it could be specified unambiguously,[11] will decide the shape. This is the static Jahn–Teller effect. (b) The two highest occupied MO's have opposite influences on a valence angle and their energies cross each other at or near the midpoint of the range of valence angle studied (accidental degeneracy). In such a case the molecular shape will be determined by the net influence of these two opposing MO's.

It should be remarked here that it is not easy to prove the validity of the above postulate on an *a priori* quantum mechanical basis. Nevertheless, using strictly qualitative arguments we shall show that the virtue of the HOMO postulate lies in rationalizing a large amount of experimental and theoretical information on different aspects of molecular geometry. It not only provides a consistent rationale for visualizing molecular shapes, but also brings considerable flexibility into a model for molecular geometry.

The important role played by HOMO in certain chemical phenomena has been recognized before.[12–14]

2. General Qualitative Techniques

(A) Guidelines for the Qualitative Construction of Symmetry-Adapted Low-Lying Polycenter LCAO–MO's of a Given Symmetry Species, Using a Valence sp Basis Set. (1) Maximum bonding[15] or least antibonding, as the case may be, between the central and terminal atoms. (2) "Lone pair(s)" on the terminal atoms. These are orbitals having as little antibonding as possible between the terminal atoms. (3) Decrease bonding, without introducing any antibonding, until a limit set by symmetry requirements for the irreducible representation is attained. (4) "Lone pair" on the central atom. This orbital is bonding or least antibonding, as the case may be, between the terminal atoms. (5) Increase antibonding between the central and the terminal atoms until a limit set by the number of MO's belonging to the given irreducible representation is attained. The terminal atoms should have as little antibonding as possible between them. (6) Check for physical validity and internal consistency among the constructed MO's according to the following rules: (a) the MO's should be linearly independent,[18] (b) antibonding should be brought in only when feeble bonding is not permissible, (c) for AH_n molecules the "lone pair" combination of AO's on the central atom should not be repeated in any other MO.

(B) Guidelines to Decide the Energy Order of the Low-Lying LCAO–MO's. (1) The energies of MO's belonging to a given symmetry species follow the order bonding < feeble bonding ("lone pair") < nonbonding < feeble antibonding < antibonding. A π-antibonding MO has a lower energy than a σ-antibonding one. (2) For MO's of one bonding type, belonging to different symmetry species, the energy order is totally (or more) symmetric < less symmetric. The central atom "lone pair" MO is flanked by an antibonding and a bonding (or less antibonding) MO of a less symmetric species. (3) The energy order for the MO's of simpler molecules is incorporated into that for the larger molecules belonging to the same point group, e.g., AH_2 (C_{2v}) $\subset AB_2$ (C_{2v}) $\subset BAAB$ (C_{2v}; see also ref 19 and 20). (4) With the possible exception of highly ionic molecules (see later), in molecules where a central atom is linked to a lighter and a heavier atom the orbital which is bonding between the central and the heavier atom will have lower energy than that which is bonding between the central and the lighter atom. Further, a "lone pair" orbital of the lighter terminal atom will have a lower energy than a similar "lone pair" orbital of the heavier terminal atom.

(11) Although degenerate MO's cannot be distinguished energetically, the direction of a chosen force might distinguish between MO's spanning, for example, an E representation. The nature of the accompanying changes in shape may then be different for the occupancy of different but energetically the same MO's. It is then possible to argue that an electron or a hole, as the case may be, will be either of the two degenerate MO's and not in a linear combination of them because the latter occupancy may decrease the Jahn–Teller stabilization energy.[10b] In case the chosen force does not distinguish between the degenerate MO's, qualitative arguments cannot predict the nature of the occupied MO.

(12) K. Fukui, "Molecular Orbitals in Chemistry, Physics and Biology," P.-O. Löwdin and B. Pullman, Ed., Academic Press, New York, N. Y., 1964, p 513.

(13) (a) R. Bhattacharya and S. Basu, *Trans. Faraday Soc.*, 54, 1286 (1958); (b) R. B. Woodward and R. Hoffmann, *Angew. Chem.*, 8, 781 (1969).

(14) (a) L. C. Cusachs, M. Krieger, and C. W. McCurdy, *Int. J. Quantum Chem., Symp.*, 3, 67 (1969); (b) R. G. Pearson, *Pure Appl. Chem.*, 27, 145 (1971).

(15) An MO is said to be bonding or antibonding between a pair of atoms A and B if their interatomic overlap is positive or negative, respectively (see ref 16 and 17). Where there is a choice between π, antibonding and σ-antibonding character of an MO the former is to be preferred.

(16) R. S. Mulliken, "Quantum Theory of Atoms, Molecules and the Solid State," P.-O. Lowdin, Ed., Academic Press, New York, N. Y., 1966, p 231.

(17) M. Cohen and R. P. McEachran, *Theor. Chim. Acta*, 12, 87 (1968).

(18) This does not ensure that the various MO's belonging to an irreducible representation will all be orthogonal. We shall, however, see that for the first three molecule classes examined here the MO's constructed according to the above prescriptions are identical in form with the corresponding *ab initio* MO's. In case of the other molecule classes the qualitative bonding characteristics of our MO's are essentially the same as the available calculated MO's.

(19) S. D. Peyerimhoff, *J. Chem. Phys.*, 47, 349 (1967); R. J. Buenker and S. D. Peyerimhoff, *Theor. Chim. Acta*, 24, 132 (1972).

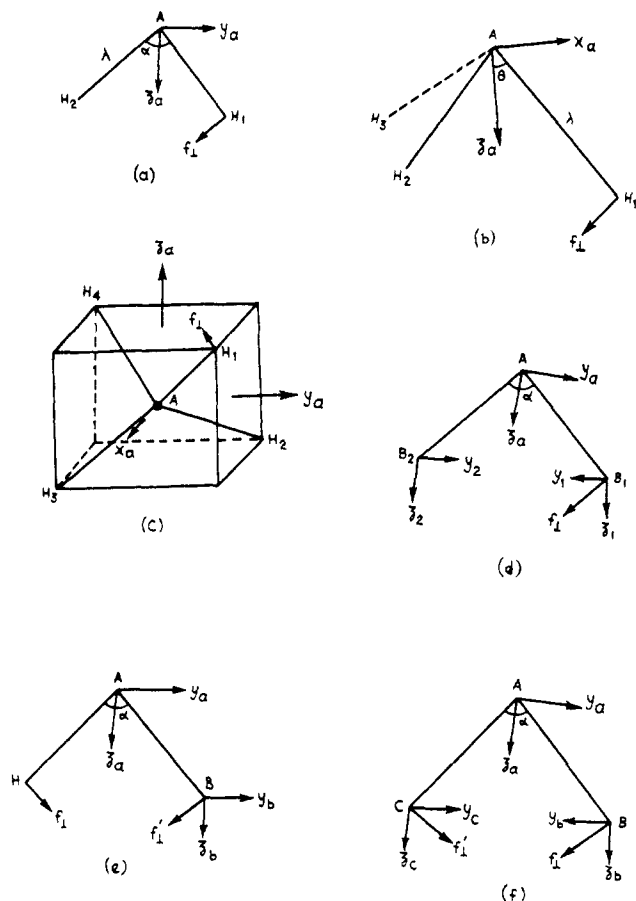(20) H. H. Schmidtke, *Int. J. Quantum Chem., Symp.*, 2, 101 (1968).

Figure 1. Coordinate system and transverse forces for six molecule classes: (a) AH_2, (b) AH_3, (c) AH_4, (d) AB_2, (e) HAB, and (f) ABC. In case of AH_3 molecules the atoms H_2 and H_3 are above and below, respectively, the plane of the paper.

(C) Guidelines to Decide Whether an MO Density Tends to Increase or Decrease a Valence Angle. It is clear from expression 3 that in obtaining the force on a nucleus due to the single-particle density in an occupied MO there are two types of terms to be considered separately: (a) *atomic forces*, resulting from the atomic density $x_p{}^2$, where x_p is an AO (pure or hybrid) on the pth nucleus, and (b) *overlap forces*, arising from the overlap distribution $x_p x_q$, p and q referring to different nuclei. These two terms may augment or attenuate each other in their influence on a valence angle. Previous force calculations[10] have shown that it is quite easy to ascertain the direction of the transverse force arising from either the atomic or the overlap density, from simple physical considerations. However, the direction of the resultant of the atomic and overlap forces is not always obvious.

(D) Choice of a Mechanical Model for Nuclear Motions. For a given class of molecules the decision about preferred shapes, depending on the number of valence electrons present, is arrived at by considering two configuration extremes for the given class and by examining the nuclear motion which takes one configuration into the other. The transverse forces on the terminal nuclei which tend to produce such motions may be used to construct a force correlation diagram (fcd) correlating the MO's in the two configuration extremes. But, unlike other correlation diagrams, the fcd can usually be constructed by considering the MO's

in one (less symmetrical) configuration extreme only since it is possible, in general, to select the other (more symmetrical) extreme to be such as to have all transverse MO forces vanish by symmetry. However, in the present paper we shall find it more convenient to employ a "shape diagram" rather than a correlation diagram, for geometrical predictions. The "shape diagram" places in separate areas the MO's tending to favor one configuration or the other while the MO's having no influence on the valence angle considered lie on the borderline separating the two areas. The area above this line corresponds to a positive transverse MO force on the terminal nuclei while the area below corresponds to a negative transverse force. The indifferent MO's do not exert any transverse force in the direction considered.

3. The Shapes of Molecules

I. AH_2 Molecules (Linear–Bent Correlation). As indicated in Figure 1, the bending of an AH_2 molecule is achieved by totally symmetric motions of the two hydrogen atoms in the molecular plane, keeping the atom A and the bond length λ fixed. The net transverse force on a proton is given as a function of the valence angle α by

$$\frac{1}{\lambda}\frac{\partial E}{\partial \alpha} = -\frac{\cos(\alpha/2)}{8\lambda^2 \sin^2(\alpha/2)} + \sum_i \eta_i \left\langle \phi_i \left| \frac{y_b}{r_b{}^3} \right| \phi_i \right\rangle \quad (4)$$

The six valence MO's of a bent ($\alpha = 60°$, say) AH_2 molecule (C_{2v}) may be constructed from valence s and p AO's grouped in Table I in the following way (see also ref 2): (i) $1a_1$, a fully bonding MO (rule 2.A.1); (ii) $2a_1$, a "lone pair" orbital localized mostly on the central atom (rule 2.A.4; rules 2.A.2 and 2.A.3 are not applicable here); (iii) $3a_1$, an MO that is strongly antibonding between A and the H atoms (feeble antibonding is not permissible as this would bring in a "lone pair" combination of AO's on the central atom (rule 2.A.6c)); (iv) $1b_2$, an MO that is bonding between the central and the terminal atoms; (v) $2b_2$, an MO which is antibonding between the central and the terminal atoms; (vi) $1b_1$, a nonbonding $p\pi$ orbital on the central atom. The MO's are represented schematically in Figures 2–4 and are in qualitative agreement with the calculated MO's[21,22] for AH_2 molecules. Using the rules 2.B.1 and 2.B.2 the MO's may be arranged in the energy order $1a_1 < 1b_2 < 2a_1 < 1b_1 < 3a_1 < 2b_2$.

From Figures 2–4 it immediately appears that both the atomic and overlap densities of the bonding $1a_1$ MO concentrate more charge inside the molecular triangle than outside it. The one-electron density of this MO would therefore exert a positive transverse force on the terminal protons. The magnitude of this force obviously decreases as the valence angle is opened up more and more, finally vanishing at the linear configuration for reasons of symmetry. This behavior of the transverse electronic force due to the $1a_1$ MO is indicated in Figure 5 which is a fcd for AH_2 molecules. For the $2a_1$ "lone pair" orbital only one term, the square of the hybrid orbital on A (Figures 2–4), gives a small resultant negative transverse force on a proton. All the overlap and other square terms in the one-electron

(21) F. O. Ellison and H. Shull, *J. Chem. Phys.*, 33, 2348 (1955).
(22) S. D. Peyerimhoff, R. J. Buenker, and L. C. Allen, *J. Chem. Phys.*, 45, 734 (1966).

Table I. Valence s and p Group Orbitals for Six Molecule Classes (see Figure 1)

Molecule class and point group	Irreducible representations	A AO's	H group AO's	B group AO's	C AO's
AH_2 (C_{2v})	A_1	s_a, pz_a	$h_1 + h_2$		
	B_1	px_a			
	B_2	py_a	$h_1 - h_2$		
AH_3 (C_{3v})	A_1	s_a, pz_a	$h_1 + h_2 + h_3$		
	E	px_a	$2h_1 - h_2 - h_3$		
		py_a	$h_2 - h_3$		
AH_4 (T_d)	A_1	s_a	$h_1 + h_2 + h_3 + h_4$		
		px_a	$h_1 - h_2 + h_3 - h_4$		
	T_2	py_a	$h_1 + h_2 - h_3 - h_4$		
		pz_a	$h_1 - h_2 - h_3 + h_4$		
AB_2 (C_{2v})	A_1	s_a, pz_a		$s_1 + s_2, py_1 + py_2,$ $pz_1 + pz_2$	
	A_2			$px_1 + px_2$	
	B_1	px_a		$px_1 - px_2$	
	B_2	py_a		$s_1 - s_2, py_1 - py_2,$ $pz_1 - pz_2$	
HAB (C_s)	A'	s_a, py_a, pz_a	h	s_b, py_b, pz_b	
	A''	px_a		px_b	
ABC (C_s)	A'	s_a, py_a, pz_a		s_b, py_b, pz_b	s_c, py_c, pz_c
	A''	px_a		px_b	px_c

density lead to positive forces. The net transverse force due to this "lone pair" orbital will therefore be positive. However, both the atomic and overlap densities in the bonding $1b_2$ orbital concentrate more charge outside the molecular triangle than inside it and would, therefore, result in a negative transverse force whose magnitude gradually diminishes as the molecule tends to linearity. The nonbonding $1b_1$ orbital does not exert any transverse force since this orbital is perpendicular to the plane of the molecule (Figures 2–4). These qualitative conclusions are confirmed by previous numerical calculations.[10]

The shape diagram for AH_2 molecules is indicated in Figures 6–8. Orbitals which result in a positive transverse force on the terminal protons will favor a decrease in the bond angle while those yielding a negative force will tend to make the molecule linear. Therefore, according to the postulate HOMO, AH_2 molecules containing one–two and five–eight valence electrons will be bent in their ground states while those with three and four electrons will be linear. It is clear that occupancy of the $1b_2$ MO by the outermost electron is a necessary condition for the linearity of an AH_2 molecule. The various conclusions about the shapes of molecules are summarized in Table II. The changes of shape, if any, of AH_2 molecules on excitation or ionization can also be explained on the basis of the shape diagram (Figures 6–8). From the present model LiH_2^+ should be bent (as is H_3^+); ab initio calculations[23,24] agree with this prediction. Further, the HeH_2^+ molecule has been calculated to be linear;[23] the first excited state of LiH_2^+ is also expected to be linear. BH_2, which is bent in the ground state, is expected to be linear[25] in the excited state $^2B_1$. Singlet carbene, $CH_2(^1A_1)$, is expected to be bent (104°, ref 25); the excited carbene, $CH_2(^1B_1)$, on the other hand, will have a greater value of the valence angle (140°, ref 25) since one electron now goes into the indifferent $1b_1$ orbital.

(23) R. D. Poshusta, J. A. Haugen, and D. F. Zetik, *J. Chem. Phys.*, 51, 3343 (1969).
(24) N. K. Ray, *J. Chem. Phys.*, 52, 463 (1970).
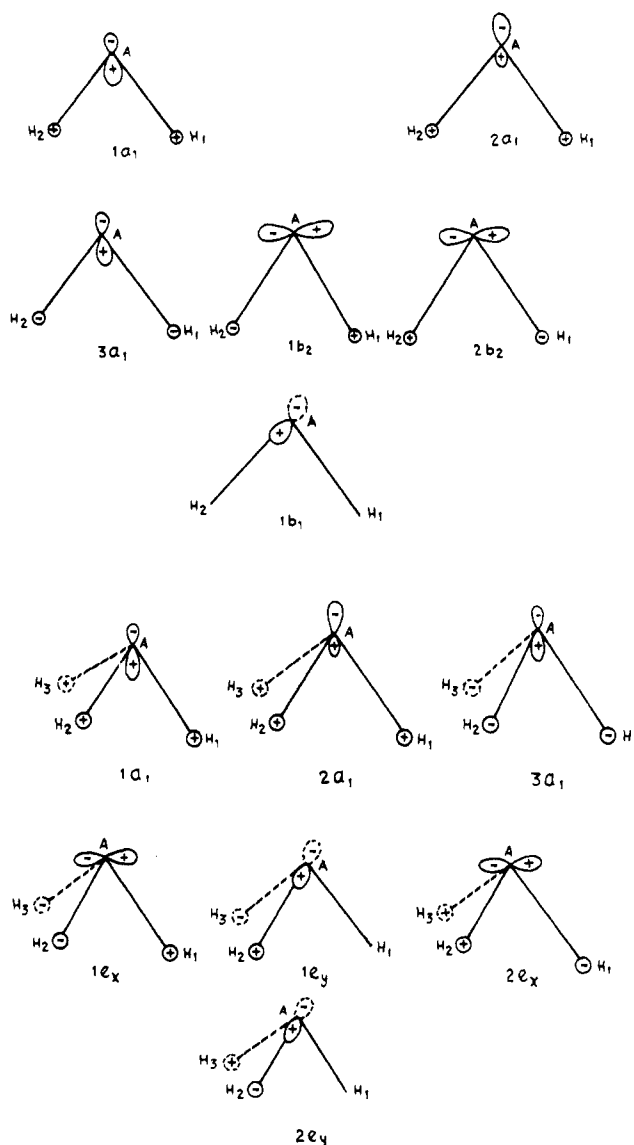(25) G. Herzberg, *Advan. Photochem.*, 5, 1 (1968).

Figure 2. Schematic MO's for AH_2 (top) and AH_3 (bottom) molecules. See also Figure 1.

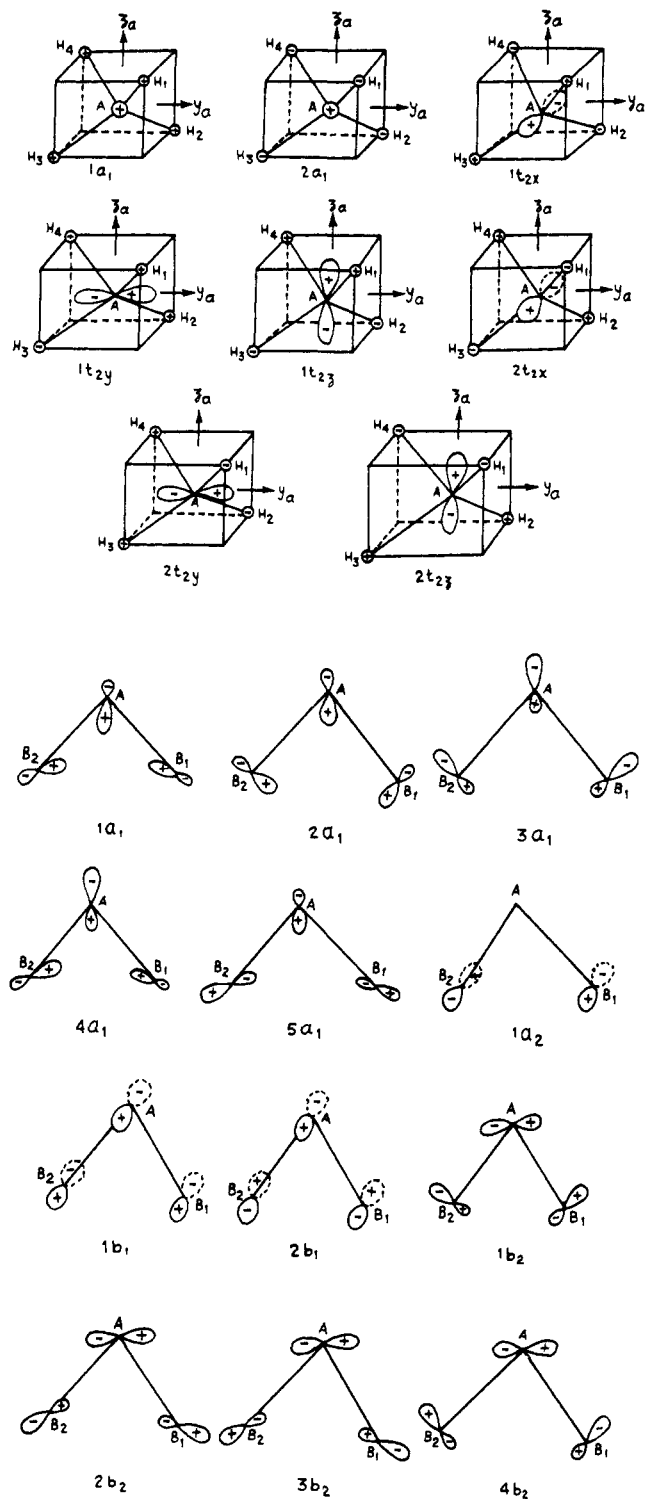*Deb / AH_2, AH_3, AH_4, AB_2, HAB, and ABC Molecules*

Figure 3. Schematic MO's for AH_4 (top) and AB_2 (bottom) molecules. The x axis for AH_4 molecules is not indicated (see also Figure 1).

Figure 4. Schematic MO's for HAB (top) and ABC (bottom) molecules.

The CH_2 triplet state, $^3B_1$, which has the same HOMO occupancy as the $^1B_1$ state is also expected to be bent with an angle close to $140°$. After much controversy,[26–29] both experimental and theoretical, about

(26) G. Herzberg and J. W. C. Johns, *J. Chem. Phys.*, **54**, 2276 (1971).
(27) G. Herzberg, *Can. J. Phys.*, **39**, 1511 (1961); *Proc. Roy. Soc. A*, **262**, 291 (1961).
(28) W. A. Lathan, W. J. Hehre, and J. A. Pople, *J. Amer. Chem. Soc.*, **93**, 808 (1971).
(29) E. Wasserman, V. J. Kuck, R. S. Hutton, and W. A. Yager, *J. Amer. Chem. Soc.*, **92**, 7491 (1970).
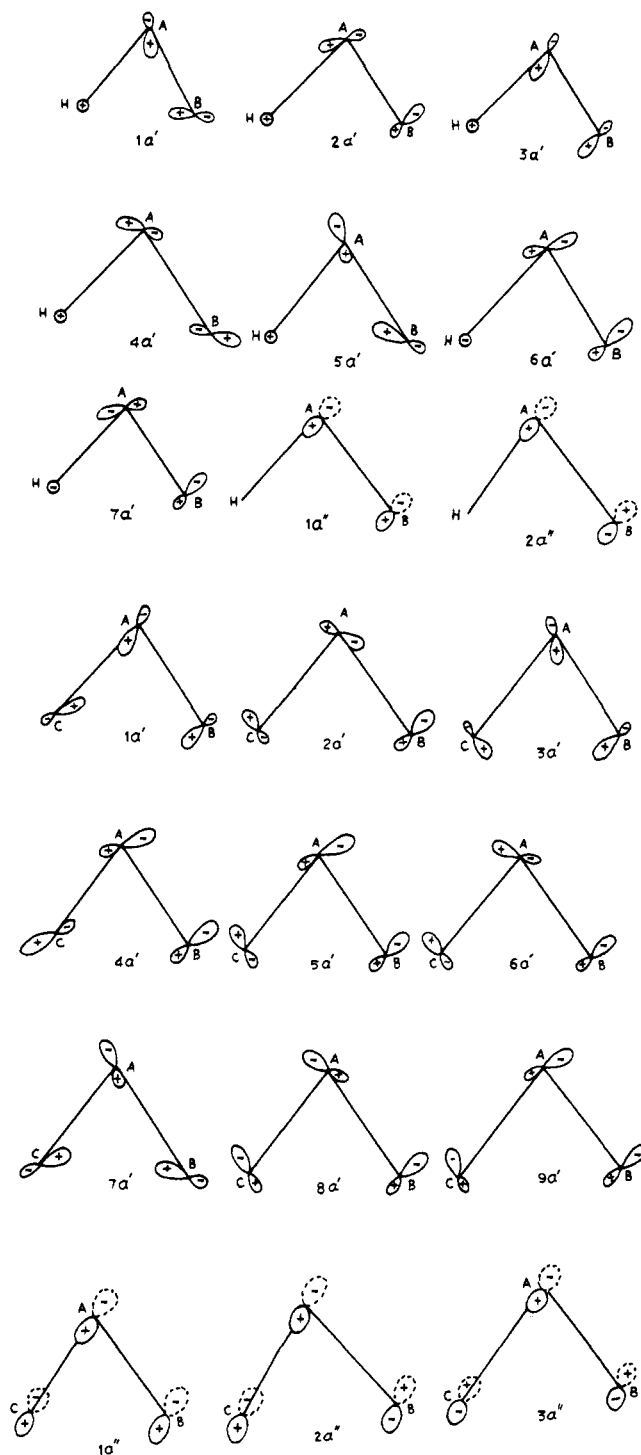
whether the CH_2 triplet and ground state is bent or linear, it now seems fairly certain that the CH_2 ground triplet is bent,[30] with an angle of $\sim 136°$. The molecules NH_2^+, NH_2 ($103.3°$), and NH_2^- ($104°$) are all expected to have more or less the same valence angle. BeH_2^- is expected to be bent. However, although both BeH_2[31] and BeH_2^+ are expected to be linear, VB calculations[23] indicate the latter to have two stable states,

(30) S. V. O'Neil, H. F. Schaefer, III, and C. F. Bender, *J. Chem. Phys.*, **55**, 162 (1971).
(31) J. J. Kaufman, L. M. Sachs, and M. Geller, *J. Chem. Phys.*, **49**, 4369 (1968).
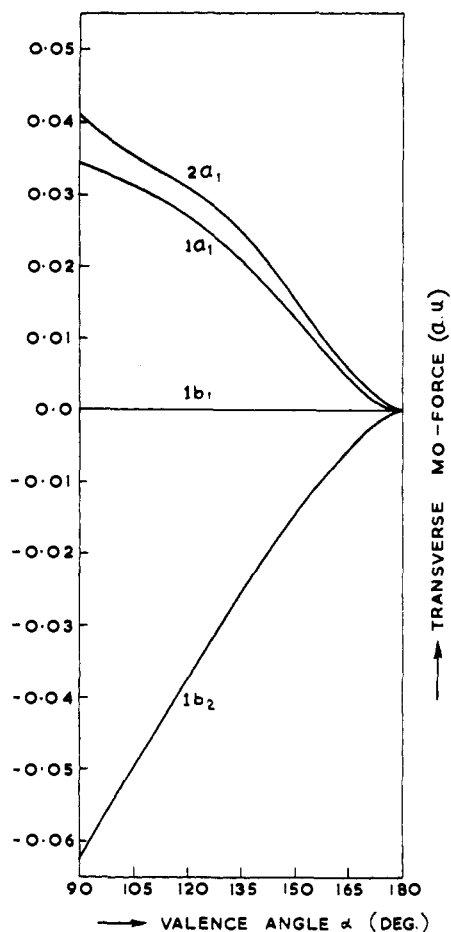
Figure 5. Force correlation diagram for AH_2 molecules, constructed with the data for the H_2O molecule taken from B. M. Deb, Ph.D. Thesis, University of Oxford, 1969.
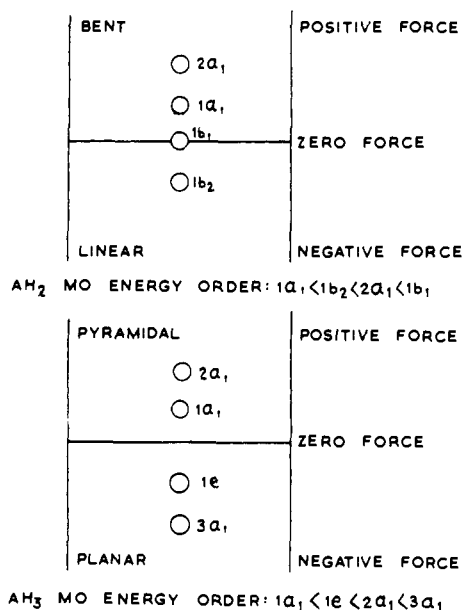

Figure 6. Shape diagrams for AH_2 (top) and AH_3 (bottom) molecules.

Figure 7. Shape diagrams for AH_4 (top) and AB_2 (bottom) molecules.
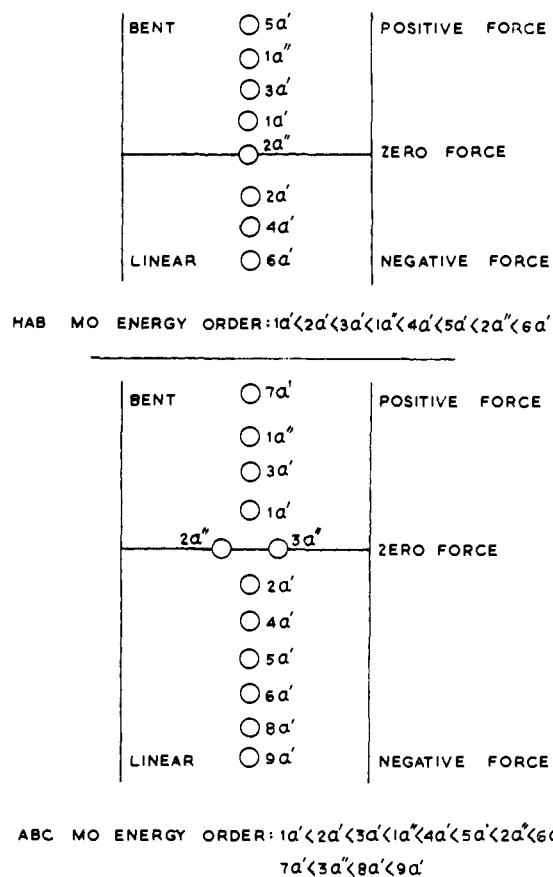
Figure 8. Shape diagrams for HAB (top) and ABC (bottom) molecules.

a linear $^2\Sigma_u^+$ and a bent $^2A_1$ state, the latter having a lower energy (cf. the situation with CH_2). The bond angle in CH_2 (104°) is expected to be less than BH_2 (131°). In another horizontally homologous series
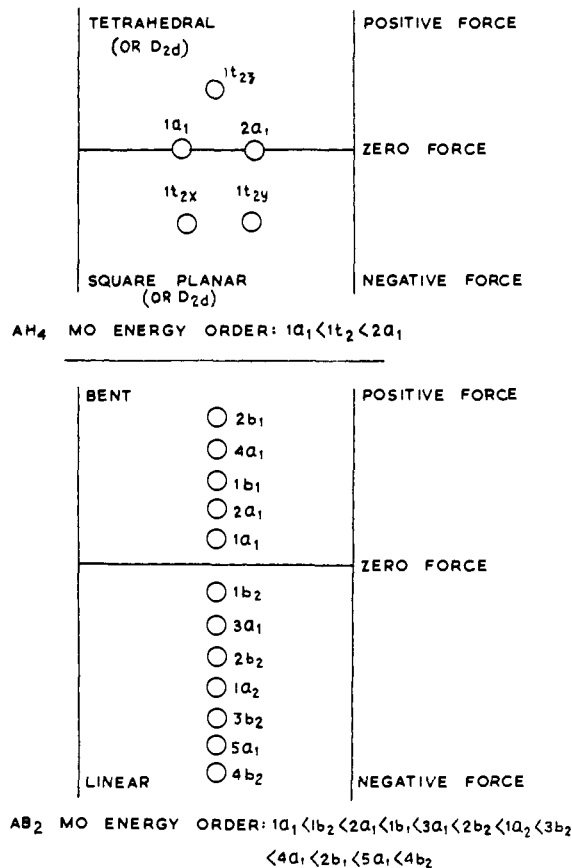
Deb / AH_2, AH_3, AH_4, AB_2, HAB, and ABC Molecules

Table II. Geometry Predictions for Six Molecule Classes (See Also Herzberg[a] and Figure 4)[e]

Molecule class	No. of valence electrons	Ground state geometry	Examples	Excited state geometry	Examples	Apparent exceptions
AH_2	1, 2	Bent	H_3^+, LiH_2^+, HeH_2^{2+}	Linear (HOMO $1b_2$)		
	3, 4	Linear	BeH_2^+, BeH_2, HeH_2^+, BH_2^+	Bent (HOMO $2a_1$)	BeH_2	BeH_2^+ (see text)
	5–8	Bent	CH_2, NH_2, OH_2, BH_2^-, BH_2, AlH_2, NH_2^+, NH_2^-	Bent[b] (HOMO $1b_1$) or linear[c] (HOMO $1b_1$)	CH_2, NH_2 (both bent), BH_2 (linear)	
AH_3	1, 2	Pyramidal		Planar (HOMO $1e$)		
	3–6	Planar	LiH_3^+, HeH_3^+, GaH_3, BeH_3, CH_3^+, BeH_3^-, BH_3	Pyramidal (HOMO $2a_1$)		
	7, 8	Pyramidal	CH_3 (?), NH_3, OH_3^+, CH_3^-, SbH_3, NH_3^+ (?), SiH_3	Planar (HOMO $4a_1$)	NH_3	CH_3, NH_3^+ (see text)
	9, 10	Planar				
AH_4	3–5	Square planar or distorted tetrahedron (D_{2d})	LiH_4^+ (D_{2d}), H_5^+ (D_{2d})			
	6	Square planar	BeH_4, BH_4^+, CH_4^{2+}			
	7	Distorted tetrahedron (D_{2d})	CH_4^+			
	8	Tetrahedral	CH_4, GeH_4, BH_4^-, NH_4^+			
AB_2	1, 2	Bent	Li_3^+	Linear (HOMO $1b_2$)		Li_2H^+ (see text)
	3, 4	Linear	He_2H^+, $BeLi_2$, Li_2H^-, Be_2H^+	Bent (HOMO $2a_1$)		
	5–8	Bent		Linear (HOMO $3a_1$)		He_3^+, Li_2O
	9–16	Linear	HF_2^-, CO_2, CO_2^+, CS_2, N_3^-, BeF_2, $HgCl_2$, $CuCl_2^-$, $Ag(NH_3)_2^+$, UO_2^{2+}, UO_2^+, MoO_2^{2+}, PuO_2^{2+}, C_3, NC_2, CN_2, $C(CH_2)_2$, $C(CO)_2$, BO_2, NO_2^+	Bent (HOMO $4a_1$ or $2b_1$)	NO_2^+, CO_2, CS_2	BaF_2, $BaCl_2$, $BaBr_2$, BaI_2, SrF_2, $SrCl_2$, CaF_2 (see text)
AB_2	17–20	Bent	NO_2^-, NO_2, ClO_2^-, ClO_2, SO_2, SCl_2, O_3, OCl_2, $SnCl_2$, PbI_2, $(CH_2)_3$, $InCl_2$, $Se(SCN)_2$, S_3^{2-}, $O(CH_3)_2$, CF_2, NF_2, ICl_2^+	Linear (HOMO $5a_1$ or $4b_2$)		
	21–24	Linear	XeF_2, I_3^-, ICl_2^-, F_3^{2-}, Cl_3			
	1, 2	Bent		Linear (HOMO $2a'$)		
	3, 4	Linear	$LiHeH^+$	Bent (HOMO $3a'$)		
	5–8	Bent		Linear (HOMO $4a'$)		LiOH (see text)
	9, 10	Linear	HCN, C_2H_2, $(CH_2)CH^+$, $HBeF$, HBO	Bent (HOMO $5a'$)	HCN	
HAB	11–14	Bent	HCO, HNO, HCF, HNF, $(CH_3)OH$, $(CH_2)CH$, HOO, $HOCl$, $HN(CN)$, $H(CH)O$, $HO(NO)$, $HN(N_2)$, $HN(CO)$	Linear (HOMO $6a'$)	HCO	
	15–16	Linear	HF_2^-			
ABC	1, 2	Bent		Linear (HOMO $2a'$)		
	3, 4	Linear		Bent (HOMO $3a'$)		
	5–8	Bent		Linear (HOMO $4a'$)		
	9–16	Linear	NNO, $BrCN$, $(CH_3)BO$, $(CH_2)(CH)Li$, $(CH_3)(CH_2)Li$, NCS, NCS^-, COS, NCO, NCO^-, CCN, $(CH_2)CO$, NNO^+, $(HN)CN$, $(HN)N_2$, $(HN)CO$	Bent (HOMO $7a'$)		
	17–20	Bent	$NOCl$, $(CH_2)(CH)Br$, $(HO)NO$, $(HF)CO$, $CH_2CHCH=(CH_2)$,[d] $ON(NO)$	Linear (HOMO $8a'$)		
	21–24	Linear	$IBrCl^-$			

[a] G. Herzberg, "Molecular Spectra and Molecular Structure. III. Electronic Spectra and Electronic Structure of Polyatomic Molecules," Van Nostrand, Princeton, N. J., 1966. [b] In this case the next lower MO is $2a_1$. [c] In this case the next lower MO is $1b_2$. [d] In the butadiene molecule the (CH_2CHCH=) fragment may be looked upon as an 18-electron molecule. Hence, its C–C–C frame will be bent. [e] The known molecular shapes are either empirical or theoretical (see text).

BH_2^- (102° calcd[32]), CH_2 (104°), NH_2 (104°), and H_2O (104.5°), bond angles are not expected to differ very much since the latter two differ from the first two only in the occupancy of the $1b_1$ orbital (Figures 6–8).

From the HOMO postulate it appears that progressive filling of a bonding or nonbonding orbital should lead to a decrease in bond length, whereas progressive filling of an antibonding orbital should result in an increase of bond length. The reason is that, for the two atoms involved, antibonding orbitals result in a depletion of charge in the binding region between the two nuclei whereas the bonding orbitals lead to a build-up of charge in this region. Further, from Figure 2 (top) it is clear that the electron density in the "lone pair" orbitals, $2a_1$ and $1b_1$, on the central atom will attract the terminal nuclei and hence the occupancy of these "lone pair" orbitals should lead to a decrease in bond length. This is exemplified by the series BH_2 (1.18 Å), CH_2 (1.11 Å), NH_2 (1.02 Å), and H_2O (0.958 Å),[33] where the A–H length gradually decreases. In the vertically homologous series H_2O (0.958 Å), H_2S (1.334 Å), H_2Se (1.47 Å), and H_2Te (1.7 Å), however, the bond length is expected to increase because of the following reason. Since the $\langle r \rangle$ values for both valence s and p AO's of the central atom increase from O to Te,[34–36] showing that the AO's become more diffuse, it is reasonable to suppose that in their hydrides there would occur a relatively lower concentration of charge in the A–H binding region as one moves from O to Te. Figure 9 indicates the relationship of $\langle r \rangle_s$ and $\langle r \rangle_p$ with the corresponding A–H bond lengths. Further, the bond angle in the series H_2O (104.5°), H_2S (92.2°), H_2Se (91°), and H_2Te (89.5°) would be expected to suffer a decrease for the following reason. Since the tail of the central atom "lone pair" sp hybrid can overlap more effectively with the hydrogenic AO's when it is more diffuse, one can expect that the bending of the nuclear framework will be more facilitated in, e.g., H_2S than in H_2O. The same type of argument may be employed to predict that the bond lengths in CH_2 (1.11 Å) and NH_2^- (1.03 Å) would be greater than those of the isoelectronic NH_2^+ (1.08 Å calcd[22]) and H_2O (0.958 Å), respectively, since in the latter two cases the $\langle r \rangle_{2s}$ and $\langle r \rangle_{2p}$ values of the central atom are smaller. It can also be expected that the stretching and bending force constants in H_2O would be greater than those in NH_2 or in H_2S.[37,38a] Deb and Coulson,[38b] as well as Pimentel, et al.,[38c] have also used $\langle r \rangle$ values of valence MO's for geometry predictions.

The HOMO postulate also helps to understand why, in passing from four-electron BeH_2 (linear) to five-

(32) L. M. Sachs, M. Geller, and J. J. Kaufman, *J. Chem. Phys.*, 52, 974 (1970).

(33) Data for bond lengths and angles are taken from L. E. Sutton, Ed., *Chem. Soc., Spec. Publ.*, No. 11 (1958); *Chem. Soc., Spec. Publ.*, Suppl., No. 18 (1965), unless otherwise mentioned.

(34) D. R. Hartree, "The Calculation of Atomic Structures," Wiley, New York, N. Y., 1957.

(35) E. Clementi, *IBM J. Res. Develop.*, Suppl., 9, 2 (1965).

(36) F. Herman and S. Skillman, "Atomic Structure Calculations," Prentice-Hall, Englewood Cliffs, N. J., 1963.

(37) G. Herzberg, "Infrared and Raman Spectra of Polyatomic Molecules," Van Nostrand, Princeton, N. J., 1966, pp 170 and 174.

(38) (a) E. B. Wilson, J. C. Decius, and P. C. Cross, "Molecular Vibrations," McGraw-Hill, New York, N. Y., 1955, pp 175–177; (b) B. M. Deb and C. A. Coulson, *J. Chem. Soc. A*, 958 (1971); (c) G. C. Pimentel, *et al.*, "Understanding Chemistry," Holden-Day, San Francisco, Calif., 1971, p 619.
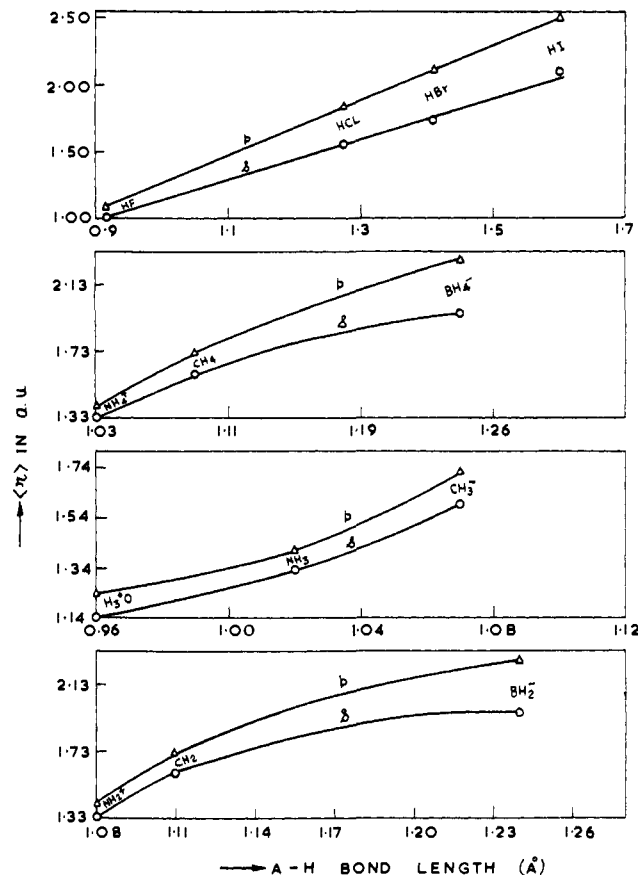
Figure 9. Correlation between bond lengths and radial expectation values for valence s and p electrons of the heavy atom in mono-, di-, tri-, and tetrahydrides. The $<p>_s$ and $<p>_p$ data are taken from Hartree[34] as well as Deb and Coulson.[38b]

electron BH_2 (bent), the addition of only *one* electron should cause the molecular shape to change so significantly.

II. AH_3 Molecules (Pyramidal–Planar Correlation). As depicted in Figure 1, the contraction or expansion of the molecular pyramid of AH_3 molecules is achieved by symmetric motions of the hydrogen atoms, keeping the atom A fixed, in the respective planes defined by the principal symmetry axis and the relevant bonds, of constant length λ. The net transverse force on each proton, as a function of the pyramidal angle θ, is given by

$$\frac{1}{\lambda}\frac{\partial E}{\partial \theta} = -\frac{\sqrt{3}\cos\theta}{3\lambda^2 \sin^2\theta} + \sum_i \eta_i \left\langle \phi_i \left| \frac{x_H}{r_H^3} \right| \phi_i \right\rangle \quad (5)$$

The seven valence MO's of a pyramidal ($\theta = 45°$, say) AH_3 molecule (C_{3v}) may be constructed from the s and p AO's in Table I as follows (see also ref 2): (i) $1a_1$, a fully bonding AO (rule 2.A.1); (ii) $2a_1$, a "lone pair" orbital localized mostly on the central atom (rule 2.A.4; rules 2.A.2 and 2.A.3 are not applicable here); (iii) $3a_1$, an MO strongly antibonding between the central and the terminal atoms (for reasons outlined with AH_2 molecules feeble antibonding is not permissible here); (iv) two e_x MO's, $1e_x$ and $2e_x$, obtained by bonding and antibonding combination, respectively, of the central atom p_x AO and the $(2h_1 - h_2 - h_3)$ group AO; (v) two e_y MO's, $1e_y$ and $2e_y$, obtained similarly, from p_y AO and the $(h_2 - h_3)$ group AO. The MO's are represented schematically (Figures 2–4) and are in qualita-
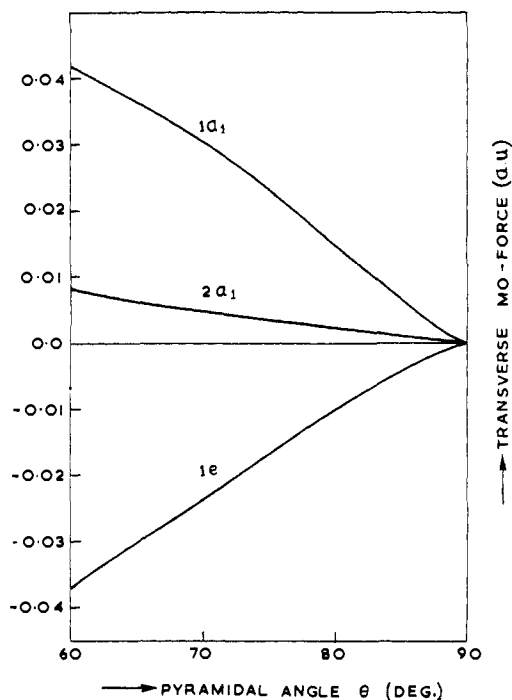
Figure 10. Force correlation diagram for AH_3 molecules, constructed with the data for the NH_3 molecule, taken from B. M. Deb, Ph.D. Thesis, University of Oxford, 1969. The 1e curve gives the resultant of $1e_x$ and $1e_y$ forces on H_1.

tive agreement with the *ab initio* MO's for NH_3.[39] Using the rules in section 2.B one can readily arrange the MO's in the energy order $1a_1 < 1e < 2a_1 < 3a_1 < 2e$.

The fcd for an AH_3 molecule is given in Figure 10. As with AH_2 molecules, the bonding $1a_1$ MO concentrates more charge inside the molecular pyramid than outside it and will, therefore, favor the pyramidal form. A similar argument like the $2a_1$ MO of an AH_2 molecule indicates that the $2a_1$ MO for AH_3 molecules would also give a positive transverse force and thus favor the pyramidal form. Similarly, just as with the $1b_2$ MO of AH_2 molecules, the $1e_x$ MO would result in a negative transverse force. The $1e_y$ orbital tends to attract H_1 (Figure 1) inward as well as to increase the $\angle H_2AH_3$. This orbital, therefore, does not favor a pyramidal form but instead tends to favor a T shape. In Figure 10 we have indicated both these orbitals to favor a planar form. If one replaces atomic densities with point charges situated at or near the respective nuclei and an overlap density with a point charge at or near the midpoint between the two nuclei involved, then one can readily see that the $3a_1$ antibonding MO should exert a negative transverse force on a terminal proton, thereby favoring a planar form.

The shape diagram for AH_3 molecules is indicated in Figures 6–8. It follows from the HOMO postulate that AH_3 molecules containing one–two and seven–eight valence electrons will be pyramidal in their ground states while those with three–six and nine–ten electrons will tend to be planar (see Table II). Obviously, a planar AH_3 molecule must have a 1e or the $3a_1$ orbital occupied by the outermost electron (see ref 40 and 41).

The shapes of ground and excited/ionized states can also be predicted on the basis of the above shape diagram. The three-electron LiH_3^+ and the four-electron HeH_3^+ should both be planar; this agrees with VB calculations.[23] The radical CH_3 is predicted to be pyramidal. Various semiempirical and *ab initio* calculations[28,42–47a] as well as experimental studies[27,48] indicate that the radical is either planar or slightly nonplanar. An extensive study of this molecule is desirable to decide clearly whether it is nonplanar or not. Another apparent exception is NH_3^+ which *ab initio* calculations predict to be planar.[47b]

As a result of progressive filling of the 1e orbitals the out-of-plane bending force constant is expected to increase in the series LiH_3^+, BeH_3, and BH_3. Similarly, because of the occupancy of the $2a_1$ "lone pair" orbital the pyramidal angle in NH_3 or H_3O^+ is expected to be smaller than that in CH_3. For reasons outlined with AH_2 molecules, the HOMO postulate also helps to explain the trend in bond lengths among the AH_3 molecules. Because bonding and "lone pair" orbitals are progressively filled up in the series LiH_3^+, BeH_3, BH_3 (1.22 Å calcd[49]), CH_3 (1.08 Å), and NH_3 (1.02 Å), the A–H bond lengths are expected to decrease in the series. However, among the vertically homologous molecules NH_3 (1.02 Å, 106.6°), PH_3 (1.42 Å, 93.5°), AsH_3 (1.52 Å, 91.8°), etc., the A–H bond length will be expected to increase since the $\langle r \rangle_s$ and $\langle r \rangle_p$ values increase from N to As. And, just as with AH_2 molecules, this increase in bond length is accompanied by a decrease in the bond angle. Similarly, in the isoelectronic CH_3^- (1.07 Å calcd[50]), NH_3 (1.02 Å), and H_3^+O (0.96 Å), the A–H bond length will decrease because of decreasing $\langle r \rangle_s$ and $\langle r \rangle_p$ values of the central atom. Further, because of progressive filling of the "lone pair" orbital, the inversion barrier in CH_3^- or NH_3 is expected to be greater than that for BH_3^- or CH_3.

A word might be said about the Jahn–Teller (J–T) effect in AH_3 molecules arising out of partial occupancy of the 1e orbitals, *e.g.*, in LiH_3^+ and BeH_3. In passing from pyramidal LiH_3^{2+} to planar LiH_3^+ the J–T effect would be expected to result in a C_{2v} structure, irrespective of whether the odd electron goes in the $1e_x$ or the $1e_y$ orbital. In the former occupancy the $Li–H_1$ (Figure 1) bond length will tend to be shorter than the other two. In the latter occupancy the $1e_y$ orbital will favor a T structure and will tend to shorten the $Li–H_2$ and $Li–H_3$ bonds compared with the $Li–H_1$ bond. In case of BeH_3 also the odd electron may be in either of the $1e_x$ and $1e_y$ orbitals and a C_{2v} structure is likely to result. If the $1e_x$ MO is occupied then the $Be–H_1$ (Figure 1) length will be shortened a little compared with the other two bonds, whereas if the $1e_y$ MO is occupied the

(39) U. Kaldor and I. Shavitt, *J. Chem. Phys.*, 45, 888 (1966).
(40) P. E. Stevenson and W. N. Lipscomb, *J. Chem. Phys.*, 52, 5343 (1970).
(41) R. E. Kari and I. G. Csizmadia, *J. Chem. Phys.*, 50, 1443 (1969).

(42) B. M. Gimarc, *J. Amer. Chem. Soc.*, 93, 593, 815 (1971).
(43) M. S. Gordon and J. A. Pople, *J. Chem. Phys.*, 48, 4643 (1968).
(44) P. C. H. Jordan and H. C. Longuet-Higgins, *Mol. Phys.*, 5, 121 (1962).
(45) D. L. Beveridge, P. A. Dobosh, and J. A. Pople, *J. Chem. Phys.*, 48, 4802 (1968).
(46) K. Morokuma, L. Pedersen, and M. Karplus, *J. Chem. Phys.*, 48, 4801 (1968).
(47) (a) A. A. Frost, *J. Phys. Chem.*, 72, 1289 (1968); (b) R. E. Kari and I. G. Csizmadia, *Int. J. Quantum Chem.*, 6, 401 (1972).
(48) M. C. R. Symons, *Nature (London)*, 222, 1123 (1969); G. Herzberg, private communication.
(49) M. E. Schwartz and L. C. Allen, *J. Amer. Chem. Soc.*, 92, 1466 (1970).
(50) B. D. Joshi, *J. Chem. Phys.*, 46, 875 (1967).

Be–H$_2$ and Be–H$_3$ lengths will be shortened, compared with the third length (see also ref 42 and 51).

III. AH$_4$ Molecules (Tetrahedral–Square Planar Correlation). In a tetrahedral AH$_4$ molecule two terminal H atoms lie in a plane at right angles to another plane containing the other two H atoms. A square planar shape is achieved by separate symmetric motions of the two pairs of terminal atoms in their respective planes. There are three such equivalent motions, one of which is depicted in Figure 1, indicating the transverse forces considered. It is necessary for our arguments that we choose *one* out of the three equivalent nuclear motions, although it does not matter which, that will take the tetrahedron to the square planar shape and *vice versa*.

The eight valence MO's of a tetrahedral (T_d) molecule may be obtained by linear combinations of valence s and p AO's (see Table I) as follows: (i) 1a$_1$, a fully bonding MO involving only the s of the central atom AO's (rule 2.A.1); (ii) 2a$_1$, an antibonding MO involving only the s of the central atom AO's (rule 2.A.5; rules 2.A.2–4 are not applicable here); (iii) *three* t$_2$ orbitals, *viz.*, 1t$_{2x}$, 1t$_{2y}$, and 1t$_{2z}$, obtained by a *bonding* combination of a central atom p orbital and an appropriate hydrogenic group orbital; (iv) *three* t$_2$ orbitals, *viz.*, 2t$_{2x}$, 2t$_{2y}$, and 2t$_{2z}$, formed by antibonding combination of a central atom p AO with an appropriate hydrogenic group AO. The MO's are represented schematically in Figures 2–4 and are in qualitative agreement with recent MO calculations.[52,53] Using the rules 2.B.1 and 2.B.2 the expected energy order of the MO's is 1a$_1$ < 1t$_2$ < 2a$_1$ < 2t$_2$. This order, however, does not match with that for CH$_4$[52] where both 2a$_1$ and 2t$_2$ are unoccupied levels and seem to be in the order 2t$_2$ < 2a$_1$. Comparison with other more recent calculations was not possible because a number of workers did not publish their results for the "virtual" orbital energies in CH$_4$, NH$_4^+$, and SiH$_4$.

Figures 1–4 reveal that both 1a$_1$ and 2a$_1$ orbitals do not yield any transverse force on the terminal protons in the given directions, due to symmetry reasons. The 1t$_{2z}$ orbital leads to a positive transverse force on the terminal protons and thus favors a nonplanar form. If one resolves the central atom p$_x$ and p$_y$ orbitals along directions on and perpendicular to the planes of motion then only the component lying on a z_a AH plane contributes to the transverse force on a proton in that plane. It then becomes easy to see that both 1t$_{2x}$ and 1t$_{2y}$ orbitals would tend to favor a planar form. These considerations are summarized in the shape diagram (Figures 6–8).

The occurrence of triply degenerate MO's in AH$_4$ molecules now makes geometrical predictions less straightforward. However, this difficulty can be dealt with in the following way. Let us imagine the tetrahedron to be flattened a little, *i.e.*, assume a D_{2d} configuration intermediate between the tetrahedral and the square planar form. This will split the threefold degeneracy of the 1t$_2$ orbitals, making the doubly degenerate "1t$_{2x}$" and "1t$_{2y}$" orbitals lie lower in energy than the "1t$_{2z}$" orbital. Therefore, seven and eight valence

electron AH$_4$ molecules will be nonplanar. Since the eight-electron molecules CH$_4$ and NH$_4^+$ are tetrahedral, one can say that other eight-electron AH$_4$ molecules such as GeH$_4$, BH$_4^-$, etc., should also be tetrahedral. But this means that seven-electron AH$_4$ molecules, such as CH$_4^+$, will assume a D_{2d} form, somewhere between the tetrahedral and the square planar (J–T effect), since there is now only one electron in the "1t$_{2z}$" orbital.[8a,28,42,51,54–56] However, six-electron molecules, *e.g.*, BeH$_4$, BH$_4^+$, CH$_4^{2+}$, etc., will tend to be square planar (see ref 8a). Molecules with three–five electrons, *e.g.*, LiH$_4^+$, H$_5^+$, etc., will have a tendency to move toward a square planar form. However, it is quite possible that because of the J–T effect this motion may stop before they reach the planar form, resulting in D_{2d} symmetry.

Because of the occupancy of the indifferent 2a$_1$ level the molecules CH$_4^-$ and NH$_4$ will also be tetrahedral. The first excited states of GeH$_4$ and BH$_4^-$ are subject to a J–T distortion. The ground tetrahedron will be flattened or elongated (D_{2d}) depending on whether a 1t$_{2z}$ or a 1t$_{2x}$/1t$_{2y}$ hole is involved. In the homologous tetrahedral molecules BH$_4^-$ (1.21–1.28 Å), CH$_4$ (1.09 Å and NH$_4^+$ (1.03 Å), the A–H bond length is expected to decrease because of decreasing $\langle r \rangle_s$ and $\langle r \rangle_p$ values of the central atom. Similarly, in the vertically homologous series CH$_4$ (1.09 Å), SiH$_4$ (1.48 Å), and GeH$_4$ (1.53 Å), the A–H bond length increases because of increasing $\langle r \rangle$ values of the AO's.

IV. AB$_2$ Molecules (Linear–Bent Correlation). As depicted in Figure 1 the directions of the transverse forces and motions of the terminal nuclei in an AB$_2$ molecule are those employed for AH$_2$ molecules. The 12 valence MO's of a C_{2v} AB$_2$ molecule ($\alpha = 60°$, say) may be constructed from valence s and p group AO's (Table I) as follows: (i) 1a$_1$, an MO having maximum bonding between A and the B atoms (rule 2.A.1); (ii) 2a$_1$, an MO which is a "lone pair" combination of AO's on the terminal atoms (rule 2.A.2); (iii) 3a$_1$, an MO which is feebly bonding between the central and the terminal atoms (rule 2.A.3); (iv) 4a$_1$, an MO which is predominantly localized ("lone pair") on the central atom (rule 2.A.4); (v) 5a$_1$, an MO that is feebly antibonding between A and the B atoms (rule 2.A.5); (vi) 1a$_2$, a π MO which is A–B nonbonding and B–B antibonding; (vii) 1b$_1$, a π orbital which is A–B bonding; (vii) 2b$_1$, a π orbital that is A–B antibonding; (ix) 1b$_2$, an MO which has maximum bonding between A and the B atoms (rule 2.A.1); (x) 2b$_2$, an MO which is a "lone pair" combination of AO's on the terminal atoms (rule 2.A.2; rules 2.A.3 and 2.A.4 are not applicable here); (xi) 3b$_2$, an MO which has feeble A–B antibonding and feeble B–B antibonding (rule 2.A.5); (xii) 4b$_2$, an MO which is A–B antibonding and feeble B–B antibonding (rule 2.A.5). The 12 MO's have been represented schematically in Figures 2–4. Although not all of our linear combinations are identical with *ab initio* or semiempirical ones[57–63] which differ from one calcu-

(51) C. A. Coulson and H. L. Strauss, *Proc. Roy. Soc., Ser. A*, **269**, 443 (1962).

(52) W. E. Palke and W. N. Lipscomb, *J. Amer. Chem. Soc.*, **88**, 2384 (1966).

(53) F. P. Boer and W. N. Lipscomb, *J. Chem. Phys.*, **50**, 989 (1969).

(54) G. S. Handler and H. W. Joy, *Int. J. Quantum Chem., Symp.*, **3**, 529 (1970).

(55) J. Arents and L. C. Allen, *J. Chem. Phys.*, **53**, 73 (1970).

(56) R. N. Dixon, *Mol. Phys.*, **20**, 113 (1970).

(57) L. M. Sachs, M. Geller, and J. J. Kaufman, *J. Chem. Phys.*, **51**, 2771 (1969).

(58) L. C. Allen and J. D. Russell, *J. Chem. Phys.*, **46**, 1029 (1967).

(59) G. V. Pfeiffer and L. C. Allen, *J. Chem. Phys.*, **51**, 190 (1969).

lation to another, the qualitative bonding characteristics of our MO's are essentially the same as those of the calculated MO's. By looking at the MO energy order for AH_2 molecules and by using the rule 2.B.3, the energy order for the first six AB_2 MO's becomes $1a_1 < 1b_2 < 2a_1 < 1b_1 < 3a_1 < 2b_2$. Using the other rules of 2.B the remaining MO's can be arranged in the full order $1a_1 < 1b_2 < 2a_1 < 1b_1 < 3a_1 < 2b_2 < 1a_2 < 3b_2 < 4a_1 < 2b_1 < 5a_1 < 4b_2$ by noting that the $4a_1$ "lone pair" orbital will be flanked by $1b_1$ and $2b_1$ as well as by $3b_2$ and $4b_2$. This order, however, is not invariant for all AB_2 molecules (see above references); in particular, the orders for $1a_2$, $3b_2$ and $5a_1$, $4b_2$ may be reversed. But, as we shall see below from the nature of the MO forces, such reversal will have no effect on our predictions of gross shapes for these molecules.

Arguments similar to those employed for AH_2 molecules show that the orbitals $1a_1$ and $1b_2$ will favor bent and linear configurations, respectively. The $2a_1$ MO will favor a bent molecule (Figures 2–4). For the antibonding $1a_2$ MO the two $p\pi$ orbitals on the terminal atoms may be regarded as being away from each other and hence this MO throws more charge outside the molecular triangle than inside it. The other two π MO's, $1b_1$ and $2b_1$, would favor a bent molecule. The $3a_1$ MO will clearly result in a negative transverse force while the $4a_1$ MO which is a "lone pair" on the central atom will generate a positive transverse force on a terminal nucleus, just as with AH_2 molecules. For the $5a_1$ MO density one square and one overlap term give a strong negative transverse force while two square terms and two overlap terms will give much smaller positive transverse forces (Figures 2–4). It will not be unreasonable if we consider the balance between the two types of forces to be somewhat on the negative side. The orbitals $2b_2$, $3b_2$, and $4b_2$ are all seen to lead to negative transverse forces on the terminal nuclei. The behavior of these MO forces parallels that of the corresponding orbital energy gradients.[59]

Table II summarizes the predictions regarding the shapes of AB_2 molecules in their ground and excited states. From the shape diagram (Figures 6–8) it appears that molecules like XeF_2 and Cl_3[64] will be linear in both their ground and first excited states. It is highly significant that most of the known bent AB_2 molecules are those containing only 17–20 valence electrons. This shows dramatically the influence of the "lone pair" MO ($4a_1$) and the $2b_1$ π MO on the valence angle as these two are the only shape-determining orbitals in such molecules. The decrease in valence angle from 17- to 20-electron molecules can also be readily explained with the help of these two MO's. The slight nonlinearity of the I_3^- and F_3^{2-} ions (in the crystal) may be due to environmental constraints and cannot be explained by the present model.[65,66]

An apparent exception to the present predictions is the hypothetical five-electron molecule He_3^+ which calculations[23] predict to be linear. A detailed orbital energy analysis for this molecule is clearly desirable. Further, the 16-electron molecules BaF_2, $BaCl_2$, $BaBr_2$, BaI_2, SrF_2, $SrCl_2$, and CaF_2 are probably bent,[67a] contrary to Walsh's and our predictions as well as to those of Gillespie. Hayes[67c] argues that for these molecules central atom d AO's participate significantly in bonding, and it is possible to explain their bent shapes on the basis of a modified Walsh diagram which incorporates such d orbitals explicitly.[67b] However, it is not our purpose to include d AO's in the present treatment although it may be said that the successes of the Walsh diagram can generally be reproduced in the force formulation. Further, the present model does not accommodate predominantly ionic molecules like the linear two-electron Li_2H^+ [42] and the linear eight-electron Li_2O molecule.[58] We shall see later that the shape of another ionic molecule, LiOH (linear), is also not in accord with the predictions for its class HAB. Ab initio calculations on molecules like LiB_2, LiBLi, BeBBe, etc., would help to decide whether the present predictions about the shapes of five–eight-electron molecules are correct. The four-electron molecule $BeLi_2$ is expected to be linear.[69]

The AB_2 shape diagram may also be employed to explain the anchor shape of ClF_3. Considering a ClF_2 fragment in the molecule one may assume than an electron from the remaining Cl–F bond is also important in deciding the shape of the ClF_2 fragment in ClF_3. The resulting 22-electron fragment is expected to be linear, like XeF_2, thus yielding a T shape for the whole molecule. However, in the T configuration the two terminal fluorine nuclei (in the fragment) "see" more electrons due to the remaining Cl–F bond. The resulting electron–nuclear attraction will cause the other two Cl–F bonds to bend a little until offset by fluorine nuclear–nuclear repulsions (see also section 4).

As explained with AH_2 molecules, the progressive filling of antibonding orbitals in a horizontally homologous series will lead to an increase in bond length, in the two series BO_2, CO_2 (1.16 Å); O_3 (1.28 Å), ClO_2 (1.49 Å). In the series CO_2 (180°, 1.16 Å), NO_2 (134°, 1.20 Å), and O_3 (116.8°, 1.28 Å) and NO_2^+ (180°), NO_2 (134°, 1.20 Å), and NO_2^- (115°, 1.24 Å) the valence angle is expected to decrease because of the progressive occupancy of the $4a_1$ orbital. As in AH_2 and AH_3 molecules this decrease in bond angle will be accompanied by an increase in bond length. In the vertically homologous series CO_2 (1.16 Å), SiO_2 (1.6 Å), OCl_2 (111°, 1.70 Å), and SCl_2 (102°, 2.0 Å), as well as O_3 (1.28 Å) and SO_2 (1.43 Å), the A–B bond length is expected to increase because of increasing $\langle r \rangle_s$ and $\langle r \rangle_p$ values of the central atom. In the last two series this bond-length increase should be accompanied by a bond-angle decrease. However, the series O_3 (116.8°) and SO_2 (119.5°) appears anomalous in this

(60) S. D. Peyerimhoff and R. J. Buenker, *J. Chem. Phys.*, **49**, 2473 (1968).

(61) C. Petrongolo, E. Scrocco, and J. Tomasi, *J. Chem. Phys.*, **48**, 407, 1500 (1968).

(62) L. Burnelle, P. Beaudouin, and L. J. Schaad, *J. Phys. Chem.*, **71**, 2240 (1967).

(63) L. Burnelle, A. M. May, and R. A. Gangi, *J. Chem. Phys.*, **49**, 561 (1968).

(64) L. Y. Nelson and G. C. Pimentel, *J. Chem. Phys.*, **47**, 3671 (1967).

(65) E. H. Wiebenga, E. E. Havinga, and K. H. Boswijk, *Advan. Inorg. Chem. Radiochem.*, **3**, 91 (1961).

(66) M. C. R. Symons, *J. Chem. Soc.*, 570 (1963).

(67) (a) L. Wharton, R. A. Berg, and W. Klemperer, *J. Chem. Phys.*, **39**, 2023 (1963). (b) The bent shapes of BaX_2, where X is a halogen atom, can also be explained by the following simple hybridization argument.[68] The Ba atom has a ground state $(6s)^2$ and its first excited state is $(6s)(5d)$. This results in two sd hybrids at right angles to each other. (c) E. F. Hayes, *J. Phys. Chem.*, **70**, 3740 (1966).

(68) C. A. Coulson, private communication.

(69) J. J. Kaufman and L. M. Sachs, *J. Chem. Phys.*, **52**, 638, 645 (1970).

regard. Similar arguments are expected to hold good for ClO_2 (118.5°, 1.49 Å) and ClO_2 (110°, 1.57 Å). In the latter cases increased occupancy of the antibonding $2b_1$ orbital decreases the bond angle and this is accompanied by an increase in bond length.

The AB_2 molecules provide a chance for examining the effects of ligand substitution on the molecular geometry. The O–X bond length in OCl_2 (1.70 Å) is expected to be larger than that in OF_2 (1.42 Å) because the ligand atom in the former case has greater $\langle r \rangle$ values. The greater diffuseness of the chlorine valence orbitals means that the terminal nuclei "see" less charge concentration between them in the $2b_1$ MO which is bonding between the terminal atoms. In other words, OCl_2 (111°) will also have a greater valence angle than OF_2 (103.3°). The same argument may be invoked to explain why the bond length in CS_2 (1.56 Å) should be larger than that in CO_2 (1.10 Å). Similarly, one can predict that the bending force constants should increase in the order of $OF_2 > OCl_2$, $NO_2^- > NO_2 > NO_2^+$, etc.

V. HAB Molecules (Linear–Bent Correlation). Figure 1 depicts the forces and coordination system adopted for HAB molecules. The nine valence MO's of a bent (α = 60°, say) HAB molecule (C_s) may be constructed from valence s and p AO's grouped in Table I as follows: (i) $1a'$, an MO that is primarily A–B bonding (rule 2.A.1); (ii) $2a'$, an MO which is primarily A–H bonding (rule 2.A.1); (iii) $3a'$, a "lone pair" orbital localized mainly on the B atom (rule 2.A.2); (iv) $4a'$, an MO which is feeble A–H and feeble A–B bonding (rule 2.A.3); (v) $5a'$, a "lone pair" orbital on the central atom (rule 2.A.4); (vi) $6a'$, an MO which is A–B bonding but mild A–H antibonding (rule 2.a.5); (vii) $7a'$, an MO which is A–H bonding but mild A–B antibonding; (viii) $1a''$, a π MO which is A–B bonding; (ix) $2a''$, a π MO which is A–B antibonding. These linear combinations are not exactly identical with ab initio[58,70,71] MO's although their qualitative bonding features are essentially similar to the ab initio orbitals.

Comparing with the MO energy order for AH_2 and AB_2 molecules, the six low-lying valence MO's for HAB molecules may readily be arranged as follows, $1a' < 2a' < 3a' < 1a'' < 4a' < 5a'$. Since the π-antibonding MO $2a''$ will have lower energy (rule 2.B.1) than the σ-antibonding MO's, $6a'$ and $7a'$, the overall energy order may be written as $1a' < 2a' < 3a' < 4a' < 5a' < 2a'' < 6a' < 7a'$. This order matches with ab initio calculations (see above references).

Figures 2–4 indicate that both the $1a'$ and $3a'$ orbitals will exert a positive transverse force on the terminal nuclei and hence will favor a bent configuration. The $2a'$ will tend to open up the valence angle, like the $1b_2$ MO of AH_2 and AB_2 molecules. The $1a''$ and $2a''$ orbitals will not exert any transverse force on the B atom. However, the $1a''$ MO will tend to pull the proton inward and thus favor the bent form. The $2a''$ MO, on the other hand, will exert very little force on the proton since the atomic and overlap forces arising from this antibonding orbital would tend to cancel each other; one can, therefore, assume that this orbital has little effect on the bond angle. The $4a'$ and

$5a'$ MO's would clearly favor the linear and bent forms, respectively. The $6a'$ MO is expected to favor the linear configuration. Comparison of these MO forces with the gradients of the Walsh–Allen curves is not quite straightforward since the calculated orbital energies do not show monotone behavior over the studied range of valence angle (see previous references). However, the energy gradients of several low-lying MO's in the Walsh–Allen diagram behave similarly as the corresponding MO forces.

Table II summarizes the conclusions about the equilibrium shapes of these molecules (see shape diagram in Figures 6–8). The occupancy of the central atom "lone pair" orbital, $5a'$, is crucial for the bent shapes of 11–14-electron molecules. As already pointed out, the dramatic change of shape from 10-electron (linear) to 11-electron (bent) molecules can be explained easily by invoking the HOMO postulate. Ab initio calculations on the shapes of one–two- and five–eight-electron molecules like HBLi, HBeN, etc., would be helpful in deciding whether our predictions for such molecules are correct. The 8-electron ionic molecule LiOH (linear) does not fit into this scheme. We see, however, that the first excited states of 8-electron and 14-electron molecules are expected to be linear. The vinyl radical ($H_2C)CH$, an 11-electron bent (HCC frame is bent) molecule, is expected to assume a linear HCC frame on ionization, i.e., in the vinyl cation ($H_2C)CH^+$. Approximate and ab initio MO calculations[28,72] justify these expectations. Similarly, the acetylene molecule, HC(CH), is expected to be linear.

Because of the progressive filling of the $5a'$ orbital the bond angle in the 12-electron molecule HNO will be less (108.6°[25]) than that in the 11-electron molecule HCO (119.5°[25]). In HCF (101.8°, 1.32 Å, ref 25), the substitution of F by Cl is expected to bring about an increase in the bond angle and bond length (103.4°, 1.69 Å, ref 25) since in HCCl the halogen atom "sees" less charge concentration inside the molecular triangle because of its higher $\langle r \rangle_s$ and $\langle r \rangle_p$ values. For the same reason the bond angle in HCF will be smaller than that in HCO. However, the bond angle difference between HCO and HCF is expected to be more than that between HCO and HNO since, as already indicated in the former case, two effects act together to reduce the $\angle$HCF. The bending force constants are expected to increase in the order HNO > HCO, HCF > HCO > HCN, HCF > HCCl, etc.

It has already been noticed that in passing from AH_2 or AB_2 to HAB molecules, substitution does not alter the MO energy order. However, substitution does bring about a profound change in the nature of the MO's. An outcome of this change is that the HAB molecules cannot be regarded as special cases of the AB_2 class; for instance, the shapes of 12-electron HAB and AB_2 molecules are exactly opposite to each other.

VI. ABC Molecules (Linear–Bent Correlation). Figure 1 depicts the coordinate system employed for ABC molecules. Of the two terminal atoms B and C, we shall take C to be the heavier. Further, in order to simplify the construction of the MO's, we shall adopt the view that the AB_2 molecules are only special (i.e., more symmetric) cases of the less symmetric ABC mole-

(70) R. J. Buenker and S. D. Peyerimhoff, *J. Chem. Phys.*, 45, 3682 (1966).
(71) D. C. Pan and L. C. Allen, *J. Chem. Phys.*, 46, 1797 (1967).

(72) R. Sustmann, J. E. Williams, M. J. S. Dewar, L. C. Allen, and P. V. R. Schleyer, *J. Amer. Chem. Soc.*, 91, 5350 (1969).
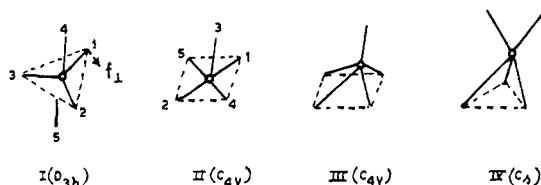
Figure 11. Four alternative shapes of an AH_5 molecule. In I the direction of the transverse force $(f_\perp)$ is in the plane containing protons 1, 2, and 3.

cules. Therefore, by enlisting help from the AB_2 MO's the 12 valence MO's of a bent ($\alpha = 60°$, say) ABC molecule (C_s) may be constructed as follows: (i) 1a′, an MO that is primarily A–C bonding (rule 2.A.1); (ii) 2a′, an MO which is primarily A–B bonding (rule 2.A.1); (iii) 3a′, a "lone pair" orbital on the B atom (rule 2.A.2); (iv) 4a′, a "lone pair" orbital on the C atom (rule 2.A.2); (v) 5a′, an orbital that is feeble A–C and feebler A–B bonding and feeble B–C antibonding (rule 2.A.3); (vi) 6a′, another MO which is feeble A–B and feebler A–C bonding and feeble B–C antibonding; (vii) 7a′, a "lone pair" orbital on the central atom (rule 2.A.4); (viii) 8a′, an orbital which is A–C bonding and A–B mild antibonding; (ix) 9a′, an MO that is A–B bonding and A–C mild antibonding; (x) 1a″, a π orbital which is A–B and A–C bonding; (xi) 2a″, a π orbital which is A–C bonding and A–B antibonding; (xii) 3a″, another π MO that is A–B and A–C antibonding. These MO's are not identical with the ones calculated by Petrongolo, *et al.*,[61] but, as in the case of AB_2 and HAB molecules, there are common qualitative bonding features. By looking at the energy order for AB_2 MO's and using the rules in section 2.B the above MO's may be arranged in the energy sequence 1a′ < 2a′ < 3a′ < 1a″ < 4a′ < 5a′ < 2a″ < 6a′ < 7a′ < 3a″ < 8a′ < 9a′. This sequence does not match the minimum Slater orbital basis calculations of Petrongolo, *et al.*,[61] for NOF whose MO energy order was found to be 1a′ < 2a′ < 3a′ < 4a′ < 5a′ < 1a″ < 6a′ < 2a″ < 7a′. This arrangement, however, does not agree with any calculated AB_2 energy order.

The schematic MO's for ABC molecules (Figures 2–4) indicate that the 1a′, 3a′, and 7a′ orbitals favor a bent configuration for these molecules while the 2a′, 4a′, 5a′, and 6a′ orbitals all favor the linear form. The bonding orbital 1a″ will exert a positive transverse force on the terminal nuclei. If one replaces the atomic charges by point charges situated at the respective nuclei and replaces an overlap charge by a point charge situated at the midpoint between the two nuclei involved, then one can see that the 2a″ orbital would lead to negative transverse forces on the terminal nuclei. This orbital will, therefore, favor a linear molecule. On the other hand, similar arguments will show that the 3a″ orbital would exert a positive transverse force on the terminal nuclei, thereby favoring a bent form. The two antibonding orbitals 8a′ and 9a′ are expected to favor the linear configuration. Owing to the unavailability of any Walsh–Allen diagram on ABC molecules one cannot compare at present these MO forces with the corresponding orbital energy gradients.

Table II summarizes the conclusions about the configurations of ABC molecules whose shape diagrams are indicated in Figures 6–8. As in HAB molecules the

occupancy of the central atom "lone pair" orbital is seen to be mainly responsible for the bent shapes of many (*e.g.*, 17–20 electron) ABC molecules. However, the HAB molecules cannot be regarded as belonging to the ABC class because the shapes of 11–14-electron molecules are predicted to be opposite for HAB (bent) and ABC (linear) molecules. The predicted shapes of five–eight-electron molecules can be checked by calculating *ab initio* the shapes of such molecules as BeLiB, BBeC⁺, etc. We notice that substitution of a B atom in AB_2 by another nonhydrogenic atom does not bring about any major change in gross shape predictions.

The bond angle in the series NOF (110°), NOCl (116°), and NOBr (117°) would be expected to increase since the increasingly diffuse halogen s and p AO's would facilitate less the bending of the nuclear framework. For the same reason substitution of one oxygen in NO_2 (134°) by a sulfur (NOS) would increase the valence angle, whereas substitution by a fluorine (NOF) would tend to decrease the bond angle.[73]

With the introduction of an extra electron in NCS the C–N (1.25 Å) and C–S (1.59 Å) bond lengths in NCS⁻ are expected to be shorter than those in NCS. A similar conclusion applies in NCCl (C–N = 1.16, C–Cl = 1.63 Å) compared with NCS, as well as in the series NCN, NCO, and NCF. The O–X bond length in the series of NOF (1.52 Å), NOCl (1.95 Å), and NOBr (2.14 Å) is expected to increase whereas the O–F bond length in NOF (1.52 Å) is expected to be smaller than the O–O length (2.21 Å) in NO_2. The central atom halogen bond length in NSBr will be larger than that in NOBr (2.14 Å). The same is expected to be true in NOF (1.52 Å) compared with NF_2 (1.37 Å).

4. Transferability of Geometry Predictions from Smaller to Higher Molecule Classes

It seems possible that the gross equilibrium shapes for higher molecule classes can be predicted on the basis of certain of their fragments belonging to smaller molecule classes. For example, the shapes of AH_4 and AH_5 molecules can be predicted on the basis of those of AH_2 molecules, while the shapes of AB_4 and AB_5 molecules can be predicted by utilizing the shapes of AB_2 molecules (for AB_3 molecules see section 3.IV).

Consider, for example, the tetrahedral–square planar correlation for AH_4 molecules, brought about by nuclear motions as described in section 3.III. The tetrahedral/D_{2d} or square planar shape of an n valence electron AH_4 molecule is determined by the bent or linear shape, respectively, of an $(n - 2)$ valence electron AH_2 fragment, since the other two A–H bonds, lying in a perpendicular plane and contributing two valence electrons, say, would have little effect on the shape of the AH_2 fragment considered. Table III shows how the geometry predictions for AH_2 molecules can be transferred to AH_4 molecules. The resulting AH_4 predictions agree with previous ones made (Table II) on the basis of the shape diagram.

Consider now the trigonal bipyramid and tetragonal pyramid correlation for AH_5 molecules. Figure 11 indicates the nuclear motions which take one configura-

(73) The extra electron in NOF would also tend to decrease the bond angle. Since these two effects act together it is reasonable to expect that the bond angle in NOF (110°) would be considerably less than that in NO_2 (134°).

Table III. Shape Predictions for Higher Molecule Classes Based on Those for Smaller Molecule Classes (See Also Table II)

Fragment	Example	No. of valence electrons	Ground state geometry	Corresponding parent molecule	No. of valence electrons	Ground state geometry	Examples
AH_2		1, 2	Bent	AH_4	3, 4	T_d/D_{2d}	See Table II
		3, 4	Linear		5, 6	Sq planar	
		5–8	Bent		7–10	T_d/D_{2d}	
AH_2		1, 2	Bent	AH_5	3, 4	Trig bipyr	CH_5^+ (?); see text
		3, 4	Linear		5, 6	Tetrag pyr	
		5–8	Bent		7–10	Trig bipyr	
AB_2	CCl_2	18	Bent	AB_4	32	T_d/D_{2d}	CCl_4, IO_4^-, SeO_4^{2-}, PO_4^{3-}, $ZrCl_4^{2-}$, $AlCl_4^-$, $HgCl_4^{2-}$, BF_4^-, BeF_4^{2-}
	SF_2	20	Bent		34	T_d/D_{2d}	SF_4
	XeF_2	22	Linear		36	Sq planar	XeF_4, BrF_4^-
AB_2	$-PCl_2$	20[a]	Bent	AB_5	40	Trig bipyr	PCl_5, $Sb(CH_3)_3Br_2$
	$-BrF_2$	22[a]	Linear		42	Tetrag pyr	BrF_5, SbF_5^{2-}

[a] This takes into account one electron from the remaining A–X bond in the plane of nuclear motion.

tion into the other; the terminal nuclei 3, 4, and 5 may be imagined to remain fixed during motions of the other two nuclei. Once again, whether an n-electron AH_5 molecule would be a trigonal bipyramid (I) or a tetragonal pyramid (II) depends on whether a corresponding $(n - 2)$-electron AH_2 fragment would be bent or linear, respectively, since two other A–H bonds lying perpendicular to the plane of nuclear motions and contributing two electrons, say, would have little effect on the shape of the AH_2 fragment considered. The resulting transferability in predictions (Table III), however, is difficult to verify. Theoretical calculations[74] on CH_5^+ try only to distinguish between the configurations I, III, and IV (Figure 11). Gole[74a] predicts the order of stability to be I > III > IV whereas others[74b] predict the stability order as IV > III > I. Since III and IV possess more bent CH_2 fragments than I, one might expect them to be more stable than I. Similar considerations apply to AB_4 and AB_5 molecules (see Table III).

5. Concluding Remarks

Table II indicates that *the predictions about gross molecular shapes, based on the HOMO postulate, are applicable even if one replaces the nonhydrogenic atoms A, B, and C by groups of atoms.* This considerably broadens the field of applicability of the present model, for this enables one to predict the shapes of fragments in larger molecules (thus having an idea of the overall shapes of these molecules) and the shapes of reactive intermediates in organic and biochemical reactions. These Walsh type predictions are applicable to any molecule that is not predominantly ionic and whose bonding can be described reasonably well in terms of valence s and p AO's. A number of transition metal compounds fit into this scheme. The bond angle variations in isoelectronic molecules belonging to different classes, e.g., (CH_4, NH_3, H_2O), (H_3^+O, H_2O), (NH_3, NH_2^-), etc., can also be predicted. In the first series, from CH_4 to H_2O, the one-electron density in the doubly filled HOMO has to pull respectively 4, 3, and 2 protons in order to preserve the "bent" shapes of the molecules. It is reasonable to expect, therefore, that in

this series bond angle would decrease from CH_4 to H_2O. The same conclusion applies to the other two series. Further, it has been seen that for five of the six molecule classes examined here the central atom "lone pair" MO disposes its one-electron density in such a way as to pull the terminal nuclei inward and thereby favor the bent (or pyramidal) configuration. The "lone pair" orbitals on the terminal atoms, however, may favor either a bent or a linear shape. Also, from Table II it appears as if tri- and tetratomic molecules having one or two valence electrons would tend to assume a less symmetrical form.

It should be noted that although the main idea in this paper, namely, the behavior of the HOMO, more than that of other MO's, is primarily responsible for deciding molecular shapes, as seems to have a sound empirical basis, the postulate stands now as a hypothesis to be tested on as many different molecules as possible. The predictive success of the model, on the basis of the symmetry-adapted HOMO, provides yet another example of the subtle way symmetry principles lurk behind chemical phenomena.

Summarizing, the present Hellmann–Feynman model, based on the behavior of the HOMO, regards molecular geometry to be determined by a combined play of the Walsh and Jahn–Teller effects and can provide an understanding about internal motions such as inversion and rotation as well as about the transferability of geometry predictions from smaller to higher molecule classes. Further, the Clinton–Rice[75] formulation of the static Jahn–Teller effect, which regards orbital degeneracies to arise from excitation or ionization, is readily comprehensible in terms of the postulate HOMO. This flexibility of the H–F model arises due to our description of the phenomenon of molecular shapes in terms of the MO's themselves rather than their energies and helps to correlate a large amount of available information on the shapes of the molecules examined.[76] With attention already focussed on the

(74) (a) J. L. Gole, Chem. Phys. Lett., 3, 577 (1969); (b) A. Gamba, G. Morosi, and M. Simonetta, Chem. Phys. Lett., 3, 20 (1969); V. Dyczmans, V. Staemmler, and W. Kutzelnigg, ibid., 5, 361 (1970); W. A. Lathan, W. J. Hehre, L. A. Curtiss, and J. A. Pople, J. Amer. Chem. Soc., 93, 6377 (1971).

(75) W. L. Clinton and B. Rice, J. Chem. Phys., 30, 542 (1959).

(76) After this work was submitted for publication, three papers by Nakatsuji[77] have appeared, dealing also with an electrostatic model for molecular shapes based on the H–F theorem. Apart from the HOMO postulate, the main difference in viewpoint between Nakatsuji's and the present model is the following. (1) Nakatsuji considers the net force on the central nucleus in a molecule whereas the present model considers the transverse electron–nuclear force on a terminal nucleus. (2) The present model obtains this transverse force as a resultant of atomic

role of the HOMO in chemical reactivity,[13b,14b] the present work on the role of HOMO in governing molecular geometry suggests that the behavior of the HOMO may provide a simple unifying principle in chemistry for understanding the structure and reactivity of molecules.

and overlap forces whereas Nakatsuji, by adopting certain approximations for the two- and three-center force integrals, splits the atomic plus nuclear repulsion force into atomic dipole (AD) and gross charge (GC) forces, while the overlap force is expresed as an exchange (EC) force. Nakatsuji's model predicts the shapes of a number of molecule classes including AH_2, AH_3, HAB, H_2AB, AB_2, ABC, and X_mABY_n molecules. The following remarks may be made regarding this model. (1) The planar shapes of 7 valence electron AH_3 molecules like CH_3, NH_3^+ etc., have been accepted rather than predicted. (2) The use of Mulliken approximation, which is rather inaccurate[78] in calculating force integrals, may be open to question. (3) For AH_3 and H_2AB molecules the vanishing of the net force (along the pyramidal axis) on A in the planar configuration does not necessarily mean that the molecule considered is planar; this out-of-plane force will always vanish in the planar configuration for symmetry reasons. Actually, for predicting the equilib-

rium shapes of such planar molecules one should choose a force in a HAH or HAB plane. (4) The fairly good numerical estimates of the pyramidal angles in CH_3^- and H_2CO (excited), based on force computations using INDO charge densities, are quite interesting in view of the well-known failure of such attempts on other molecules using *ab initio* densities.[9,10a] Since a major source of trouble in *ab initio* force computations is inner-shell polarization, the neglect of core polarization in CNDO/2 and INDO densities could mean that such densities may be more useful for force computations on molecules than the corresponding *ab initio* densities, as far as equilibrium shape predictions are concerned.

(77) H. Nakatsuji, *J. Amer. Chem. Soc.*, **95**, 345, 354, 2084 (1973).
(78) B. M. Deb, *Proc. Indian Nat. Sci. Acad.*, *Sect. A*, **37**, 349 (1971).

A Simple Mechanical Model for Molecular Geometry Based on the Hellmann-Feynman Theorem. II. HAAH, BAAB, AB₃, H₂AB, and B₂AC Molecules

B. M. Deb,[*1a] **P. N. Sen,**[1b] **and S. K. Bose**[1b]

Contribution from the Departments of Chemistry, Indian Institute of Technology, Bombay, India, and the University College of Science, Calcutta, India. Received March 6, 1973

Abstract: The simple model for molecular geometry proposed in an earlier paper (part I) has been applied to five more molecule classes. The postulate that *the gross equilibrium molecular shapes are determined primarily by the behavior of the highest occupied molecular orbital* (HOMO) is successful in making geometry predictions for the above five molecule classes. These Walsh-type predictions seem to work well even if one replaces the nonhydrogenic atoms by groups of atoms. The change of shape of one molecule on being added to another molecule, *e.g.*, in $BF_3 \leftarrow NH$, can also be predicted.

In part I (hereafter referred to as I)[2] a simple mechanical model for molecular geometry, based on qualitative interpretations drawn from the Hellmann-Feynman (H-F) theorem, was proposed. The general principles of the method were illustrated with six molecule classes: AH_2, AH_3, AH_4, AB_2, HAB, and ABC. In this paper we examine five more molecule classes and show that the model is successful in predicting the gross shapes and certain bond angle and bond length variations in these molecules also (see ref 76 in I).

The Shapes of Molecules

1. HAAH Molecules (Linear-Bent and Planar-Nonplanar Correlations). Planar bent HAAH molecules may assume two forms, cis and trans. In order to decide whether a planar HAAH molecule will adopt a linear or a nonlinear form, it will be sufficient to consider correlations between the cis form and the linear form. This refers to a change in the angular variable θ

(1) (a) Indian Institute of Technology; (b) University College of Science.
(2) B. M. Deb, *J. Amer. Chem. Soc.*, **96**, 2030 (1974).

(Figure 1a) with nuclear motions. Correlations involving a change in the dihedral angle will be considered later. The bending of the molecule is achieved by symmetric motions of the hydrogen atoms in the molecular plane, keeping the two A atoms and the A-H length fixed.

By using the rules given in I the ten valence MO's of a cis (C_{2v}) HAAH molecule ($\angle H_1AZ_1 = 30°$, say) may be constructed from appropriate s and p group AO's (see Table I) as follows: (i) $1a_1$, an MO that is A-A and A-H bonding; (ii) $2a_1$, an MO that is A-A bonding and feeble A-H bonding; (iii) $3a_1$, an MO which is feeble A-A bonding and feeble A-H antibonding (this may also be taken as a "lone pair" combination of AO's on the heavier atoms); (iv) $4a_1$, an MO that is mild A-A bonding and A-H antiboding; (v) $1b_1$, a π MO which is A-A bonding; (vi) $1a_2$, another π MO which is A-A antibonding; (vii) $1b_2$, an MO that is A-H bonding and feeble A-A antibonding; (viii) $2b_2$, an MO which is feeble A-H bonding and feeble A-A antibonding; (ix) $3b_2$, an MO which is feeble A-H and feeble A-A antibonding (this may also be taken as a "lone pair" combination of AO's on the heavier atoms); (x) $4b_2$,